Supplementary information
B. Supplementary figures

a

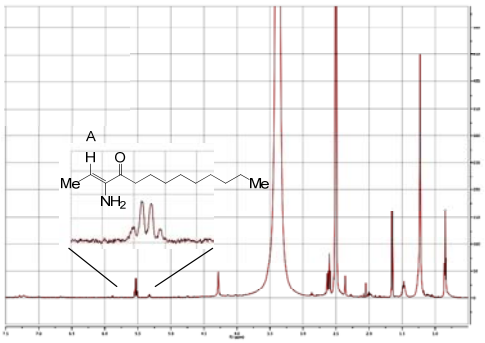

b

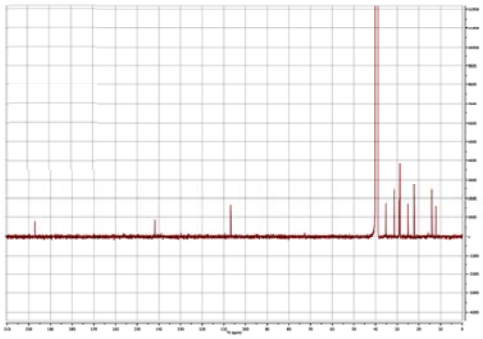

c

Comparison of ^{1}H-NMR Data for Synthetic and Enzymatic Ea-CAI-1.

Synthetic Ea-CAI-1 ^{1}H-NMR	Enzymatic Ea-CAI-1 ^{1}H-NMR
5.53 (q, *J* = 7.1 Hz, 1H)	5.53 (q, *J* = 7.1 Hz, 1H)
4.31 (s, 2H)	4.28 (s, 2H)
2.60 (t, *J* = 7.3 Hz, 2H)	2.60 (t, *J* = 7.4 Hz, 2H)
1.65 (d, *J* = 7.0 Hz, 3H)	1.65 (d, *J* = 7.1 Hz, 3H)
1.53-1.41 (m, 2H)	1.52-1.41 (m, 2H)
1.30-1.17 (m, 12H)	1.31-1.13 (m, 12H)
0.85 (t, *J* = 6.4 Hz, 3H)	0.85 (t, *J* = 6.9 Hz, 3H)

d

Comparison of ^{13}C-NMR Data for Synthetic and Enzymatic Ea-CAI-1.

Synthetic Ea-CAI-1 ^{13}C-NMR	Enzymatic Ea-CAI-1 ^{13}C-NMR
197.1	197.2
141.8	141.8
106.9	106.9
35.2	35.2
31.4	31.4
29.0	29.0
29.0	29.0
28.8	28.8
25.1	25.1
22.2	22.2
14.0	14.1
12.2	12.2

Figure S1 | Ea-CAI-1 structure. The product from *in vitro* reactions using SAM and d-CoA precipitated at high concentration. Following centrifugation, the pellet was resuspended in Deuterated DMSO (d_6-DMSO) and subjected to proton-NMR (a) and carbon-NMR (b) studies. The distinct single spectrum of quartet peaks in panel a (enlarged) indicates a single proton at the C2 position (labeled 'A' in panel a), indicative of the Ea-CAI-1 structure. The Ea-CAI-1 structure was confirmed with total synthesis (c, d). Note, these data also appear in the supplement to Ng et al. (reference 15, main text) to support the structural determination and chemical synthesis of Ea-CAI-1.

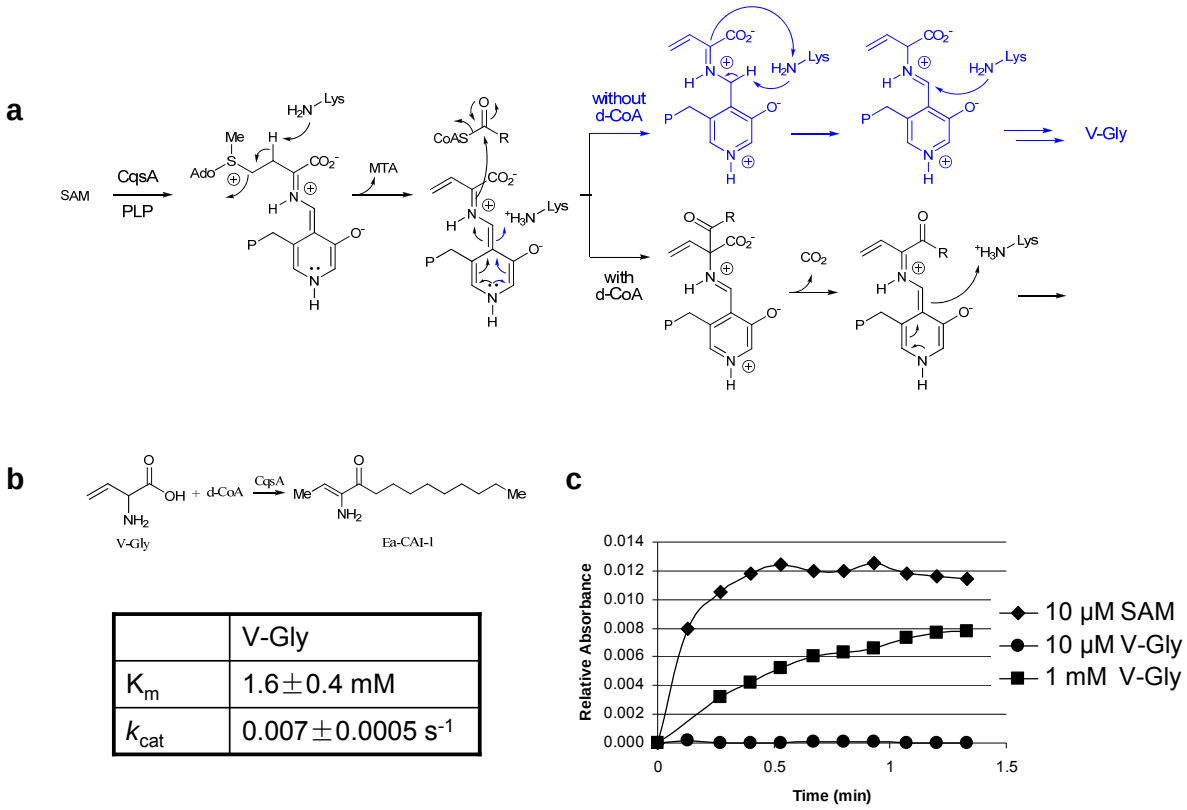

	V-Gly
K_m	1.6±0.4 mM
k_{cat}	0.007±0.0005 s^{-1}

Figure S2 | Reaction mechanism of CqsA with SAM. CqsA catalyzes the fragmentation of SAM in the absence of d-CoA (a, upper scheme). This scheme is adapted from studies on the ACCS enzyme (*1*). (b) Reaction with V-Gly and d-CoA produced an active product (molecular ion 212.2009) presumably Ea-CAI-1. No active product was observed in the reaction using Cy-Gly. Kinetic studies with 100 μM d-CoA and various concentrations of V-Gly were carried out with 1 μM CqsA as described in Methods. Kinetic analysis demonstrated that V-Gly has a significantly higher K_m and much lower k_{cat} than does SAM, indicating that SAM, and not V-Gly is the initial CqsA substrate. When both SAM and d-CoA are supplied in the CqsA reaction, V-Gly production is not detected by HRMS. (c) PLP-quinonoid intermediate formation was monitored with 1 μM CqsA and 10 μM SAM (diamonds), 10 μM V-Gly (circles) or 1

mM V-Gly (squares). At each time point, relative absorbance at 530 nm was calculated by subtracting the initial absorbance at time zero. SAM shows a significantly higher rate of formation of the PLP-quinonoid intermediate than does V-Gly. Indeed, the results with 1 mM V-Gly are included in the figure for comparison to highlight the slow rate of intermediate formation when 10 μM V-Gly is used in the reaction.

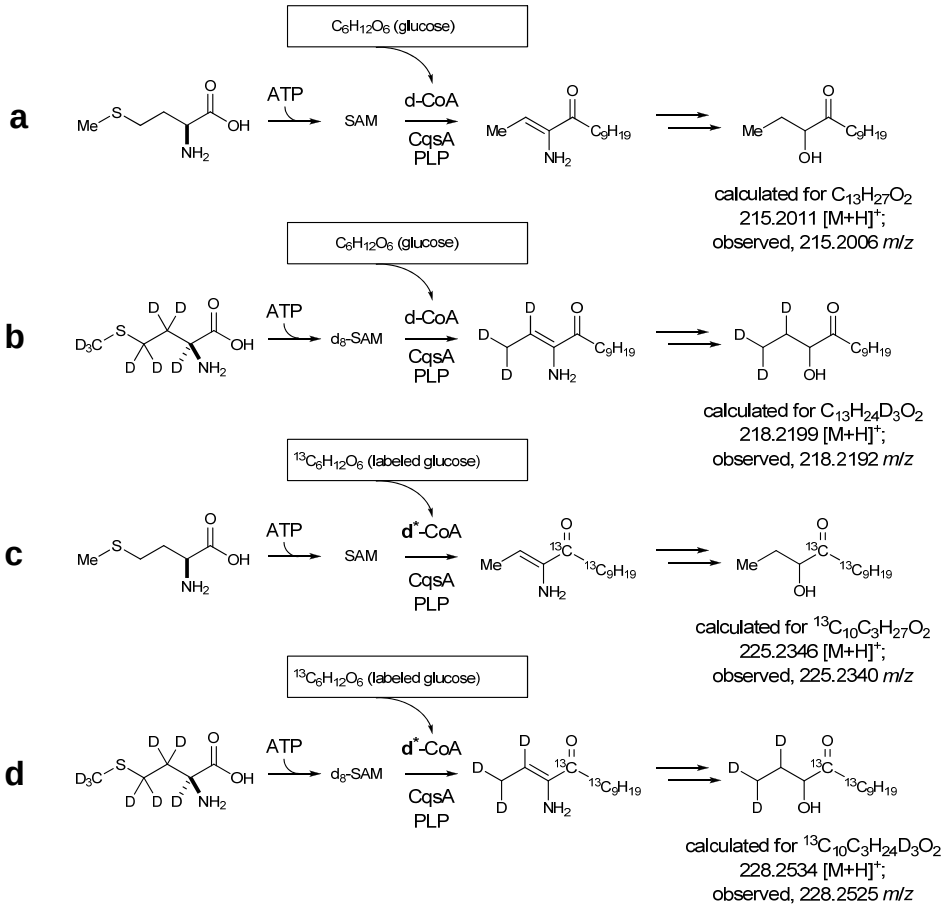

Figure S3 | Schematic illustration of labeling experiments. Supplements of L-methionine and glucose (a), d_8-L-methionine and glucose (b), L-methionine and ^{13}C-glucose (c), and d_8-L-methionine and ^{13}C-glucose (d) in the growth medium are indicated. Proton and carbon atoms from L-methionine or d_8-L-methionine *via* synthesis of SAM are incorporated into the head group of Ea-CAI-1 molecules. Due to the unsaturation in the head group, three (not four) proton/deuterium atoms are incorporated into Ea-CAI-1 and therefore into CAI-1. Protons and carbons from glucose/^{13}C-glucose are incorporated into the tail of Ea-CAI-1 therefore into the tail of CAI-1.

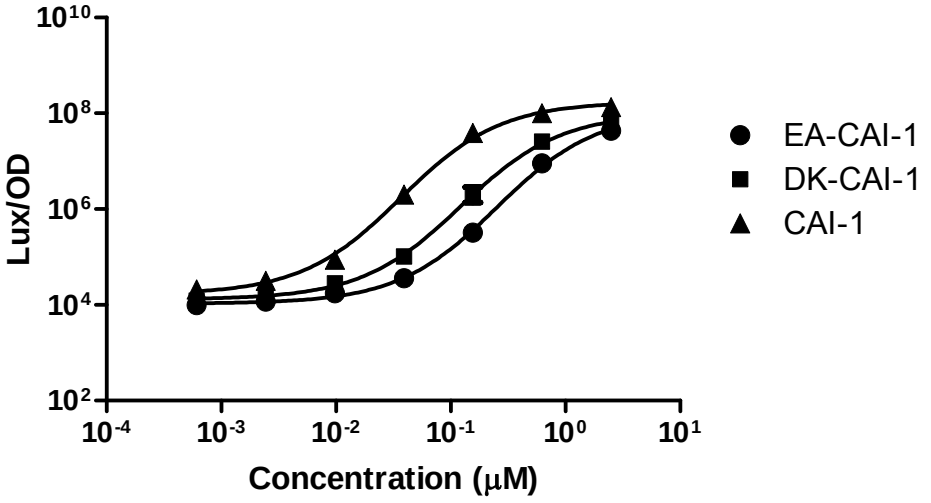

Figure S4 | Preferences of the CqsS* receptor for CAI-1 related molecules.

The CqsS* receptor prefers CAI-1 (triangles) and DK-CAI-1 (squares) over Ea-CAI-1 (circles).

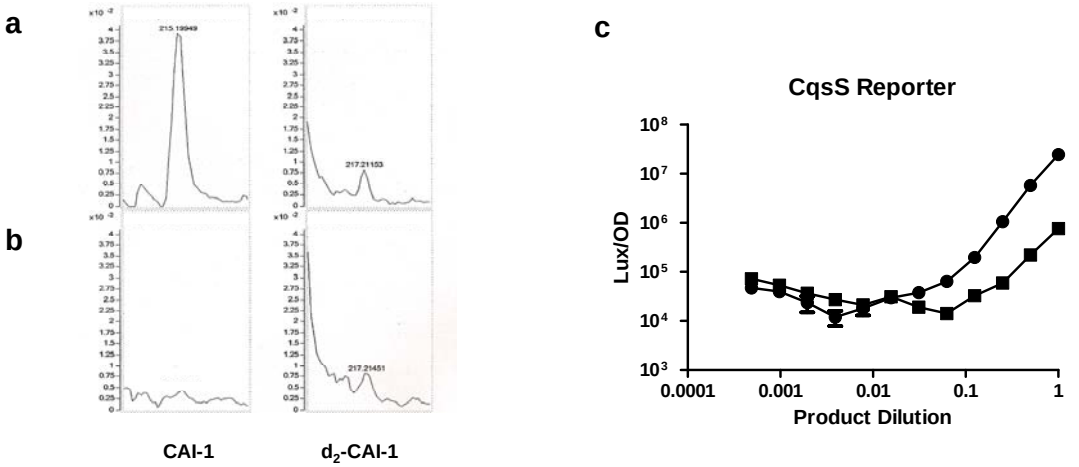

Figure S5 | Recombinant VC1059 protein converts DK-CAI-1 to CAI-1. Reactions with purified recombinant VC1059 protein and 100 μM DK-CAI-1 with (a) and without (b) 500 μM NADPH were incubated at room temperature for 30 min. Products were extracted and subjected to HRMS analysis. CAI-1 and the internal standard d_2-CAI-1 are indicated. (c) Bioassays with products with and without NADPH (circles and squares, respectively) were also performed using the wild type CqsS reporter strain.

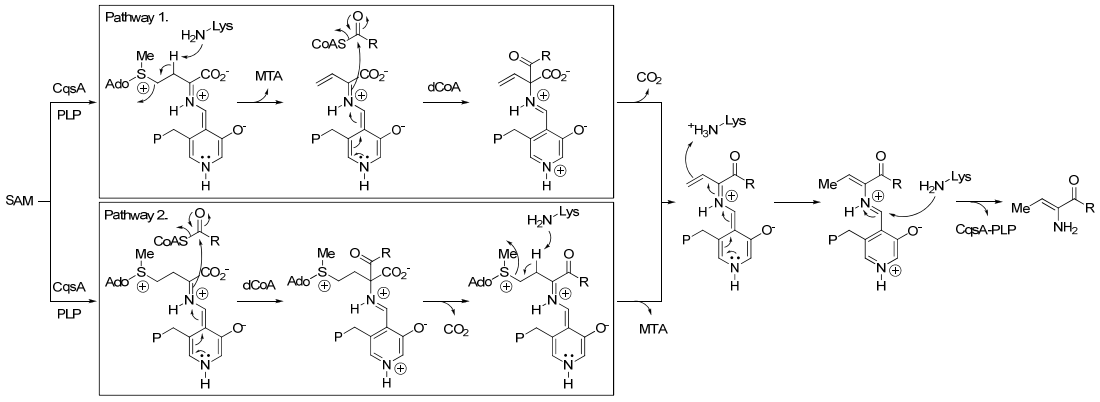

Figure S6 | Two possible schemes for the reaction that produces Ea-CAI-1. The upper scheme shows that elimination of SAM is followed by the aminotransferase reaction with d-CoA. The lower scheme shows the aminotransferase reaction with d-CoA occurs initially with the release of CoA, followed by the elimination reaction that releases MTA. Our finding of V-Gly production in the absence of SAM leads us to propose that the upper scheme is correct (main text) but we do not exclude the possibility shown in the lower scheme.

B. Supplementary tables

Table S1 | Strains list

The following *V. cholerae* strains were derived from *V. cholerae* C6706str2 (*2*)		
Strain	Genotype	Plasmid
MM920	Δ*cqsA*, Δ*luxQ*	pBB1 (*luxCDABE* from *V. harveyi*)
WYZ682	Δ*cqsA*, Δ*luxQ*, *cqsSW104AS107A (cqsS*)*	pBB1
WYZ779	Δ*vc1059*	
WYZ764	Δ*cqsA*, Δ*vc1059*	
WYZ783	Δ*cqsA*, Δ*vc1059*	P_{tac}-*vc1059*
WN1883	Δ*vca0301*	
WN1875	Δ*vc1059*, Δ*vca0301*	
WYZ791	Δ*cqsA*, Δ*vca0301*	
WYZ793	Δ*cqsA*, Δ*vc1059*, Δ*vca0301*	
E.coli BL21(DE3) was used as the parent to construct the following strains		
Strain	Plasmid	
WYZ1522	pET28b-*vc1059*	
WYZ1531	pET28b-*vc2021*	
WYZ1533	pET28b-*vca0301*	
WYZ1535	pET28b-*vc1591*	
WYZ1537	pET28b-*vca0691*	
WYZ1539	pET28b-*vca1108*	
WYZ1541	pET28b-*vc0979*	
WYZ1543	pET28b-*vca1057*	
E. coli BW25113 Δ*metE::kan* from the KEIO collection (*3*) was used as the parent to construct the following strain		
WYZ1455	P_{tac}-*cqsA*	

C. Supplementary methods

Over-expression and purification of VC1059 and homologs

Recombinant VC1059 and homologous proteins were over-expressed in *E. coli* BL21 (DE3) cells grown in LB medium containing 100 μg mL^{-1} kanamycin. Protein expression was induced with 100 μM IPTG when the OD_{600} of cells reached 0.8. Cells were grown for an additional 5 hours and harvested by centrifugation. After resuspension in lysis buffer (50 mM Tris pH 8.0, 200 mM NaCl, 20 mM imidazole), cells were lysed under 15,000 psi. Cleared fluids from lysates were passed over a Hi-Trap Chelating column (GE healthcare) charged with Ni^{2+} ion. Following washing with lysis buffer, proteins were eluted with an imidazole gradient. Protein purities were examined by SDS-PAGE followed by Coomassie brilliant blue staining and found to be ~95% pure. Following dialysis against the lysis buffer lacking imidazole, proteins were stored at -20 ^{o}C in 50 mM Tris pH 8.0, 200 mM NaCl with 30% (v/v) glycerol. Protein concentrations were determined using the Bio-rad protein assay.

High resolution mass spectrometry experiments

For HRMS studies, 100 μL samples were diluted in 100 μL HRMS solvent (9:1 (v/v) ACN: H_2O with 0.1% (v/v) formic acid) and injected into an Agilent 1200-series electrospray ionization – time-of-flight (ESI-TOF) high resolution mass spectrometer in the positive ESI mode.

References

1. Feng, L., and Kirsch, J. F. (2000) L-Vinylglycine is an alternative substrate as well as a mechanism-based inhibitor of 1-aminocyclopropane-1-carboxylate synthase, *Biochemistry 39*, 2436-2444.
2. Thelin, K. H., and Taylor, R. K. (1996) Toxin-coregulated pilus, but not mannose-sensitive hemagglutinin, is required for colonization by *Vibrio cholerae* O1 El Tor biotype and O139 strains, *Infection and immunity 64*, 2853-2856.
3. Baba, T., Ara, T., Hasegawa, M., Takai, Y., Okumura, Y., Baba, M., Datsenko, K. A., Tomita, M., Wanner, B. L., and Mori, H. (2006) Construction of *Escherichia coli* K-12 in-frame, single-gene knockout mutants: the Keio collection, *Molecular systems biology 2*, 2006 0008.